JOURNAL OF GEOPHYSICAL RESEARCH, VOL. 106, NO. A3, PAGES 3751–3757, MARCH 1, 2001

Geospace Environment Modeling (GEM) magnetic reconnection challenge: MHD and Hall MHD - constant and current dependent resistivity models

A. Otto

Geophysical Institute, University of Alaska, Fairbanks

Abstract. The work is part of several papers investigating two-dimensional magnetic reconnection in the same initial configuration with different plasma approximations. The present work compares the results of magnetic reconnection in this configuration using constant and current dependent resistivity models in the framework of traditional MHD and Hall MHD. The results can be summarized as follows. For constant resistivity the effects of diffusion or the formation of a long thin current layer limit the reconnection rate. Current dependent resistivity models result in enhanced reconnection rates in all considered cases. In these cases, reconnection is faster by a factor of 2 in the Hall MHD approximation compared to the traditional MHD. The maximum reconnection rate for the Hall MHD for all current dependent resistivities is ~ 0.2 and appears largely independent of the model specifics and the initial perturbation.

1. Introduction

Magnetic reconnection plays a fundamental role in many space and laboratory plasma systems [e.g., *Drake*, 1995; *Lee*, 1995; *Schindler*, 1995; *Sonnerup et al.*, 1995]. One of the basic unresolved problems is the physics of the diffusion region which determines the magnetic reconnection rate. Results presented in this work are based on a traditional MHD and a Hall MHD approach and are obtained as part of the Geospace Environment Modeling (GEM) reconnection challenge in an effort to clarify the physics of the diffusion region for a particular two-dimensional initial configuration. This work is accompanied by a series of other simulation papers that approach the same problem with different plasma approximations [*Hesse et al.*, this issue; *Pritchett*, this issue; *Shay et al.*, this issue] or study different aspects of the MHD and Hall MHD dynamics [*Birn and Heese*, this issue; *Ma and Bhattacharjee*, this issue; *Shay et al.*, this issue]. A description of the initial configuration, a summary of all results of the GEM reconnection challenge, and conclusions based on the comparison of the various results is presented in a separate summary paper [*Birn et al.*, this issue]. We will refer to this paper as GEMSUM.

We use the term Hall MHD to address a fluid approach which is mostly identical to MHD but includes in addition the hall term in Ohm's law (and in our approach an isotropic electron pressure term). Different from the full two-fluid approach, the Hall MHD approximation does not include finite electron inertia.

Paper number 1999JA001005.
0148-0227/01/1999JA001005$09.00

The main emphasis of this paper is to clarify the different plasma dynamics which play a role in the traditional MHD approach and the Hall MHD approximation. A main result consistent with other work in the reconnection challenge is a strongly enhanced reconnection rate of ~ 0.2 compared to the traditional MHD. This result is obtained in various plasma approximations (GEMSUM). A crucial question is to what extent it depends on the chosen parameters and on the particular initial and boundary conditions. A large magnetic reconnection rate also presents limitations to the numerical method and the parameters used for such a study.

Section 2 will briefly summarize the numerical method to solve the two-dimensional equations in the chosen plasma approximations. Section 3 first presents a discussion of the numerical and parameter limitations which not only apply to the MHD and Hall physics but to any method which employs a resistive term to model the considered problem. We then try to clarify the influence of the initial condition and finally will compare the different basic cases considered in this work. Section 4 will summarize the results and present conclusions from them.

2. Numerical Method

The initial configuration chosen for the study consists of a Harris current sheet with a magnetic perturbation to trigger magnetic reconnection (GEMSUM). The total width of the current sheet is the ion inertia length, and all length scales in the results presented below are measured in units of the ion inertia scale. Similarly velocities are measured in units of the Alfvén speed, and time is normalized to the Alfvén transit time for the ion inertia length as outlined in the summary paper.

The MHD results in this study are obtained with a two-dimensional MHD code which has been derived from a code originally developed by *Birn* [1980] and has been applied in two- and three-dimensional versions to a variety of space plasma problems including magnetic reconnection, Kelvin-Helmholtz instabilities, and pressure pulses [e.g., *Otto*, 1990; *Otto et al.*, 1995; *Otto*, 1995; *Chen et al.*, 1997]. A version including the hall dynamics has been derived for magnetosphere–ionosphere interaction [*Birk and Otto*, 1996, 1997]. The basic equations that are integrated in this method consist of the full set of resistive MHD equations [e.g., *Birn*, 1980]. The integration uses a leapfrog method which is of second order accuracy in space and in time [e.g., *Potter*, 1973].

The Hall MHD code has been derived from this MHD code by an appropriate modification of Ohm's law, i.e., including a Hall and an electron pressure term. Different from the coordinate system used in (GEMSUM), we use x normal to the current layer and z along the current layer (i.e., x and z are reversed). For the simulation we make explicit use of the symmetry of the system at $x = 0$ which makes it sufficient to compute only half of the entire domain. All two-dimensional plots in this work show half of the system, and the full system is obtained by appropriately mirroring this half.

For most MHD and Hall MHD computations, 43 grid points along the x direction ($x_{\min} = 0$, $x_{\max} = 6.3$) proved sufficient using a nonuniform grid with a maximum resolution between $\Delta_x = 0.05$ and $\Delta_x = 0.025$ at $x = 0$. We use 123 grid points in the z direction for the MHD cases yielding a resolution of about $\Delta_z \approx 0.2$. For the Hall MHD dynamics we used the same grid in the x direction but increased the number of grid points along z by a factor of 2 yielding $\Delta_z = 0.1$.

A problem of the Hall dynamics has been a rather turbulent evolution of the system. This turbulence appears at least in part initiated by the initial perturbation that generates fast mode waves (in addition to the reconnection flow pattern), which seem to provide a seed for small-scale turbulence developing at the boundary of the current layer. We could damp the initial fast waves effectively by using a relatively large background resistivity outside the initial current layer. This resistivity did not overlap with the current region and was highly effective to reduce the problem of the small-scale turbulence.

For the current dependent resistivity we used the following models:

$$\eta(j) = \kappa(j^2 - j_c^2)S(j - j_c), \quad (1)$$

$$\eta(j) = \kappa\sqrt{j^2 - j_c^2}S(j - j_c), \quad (2)$$

$$\eta(j) = \kappa(j - j_c)S(j - j_c), \quad (3)$$

with $\kappa = 0.1$, $j_c = 2.2$, and a step function $S(x)$ which is unity for $x \geq 1$ and zero otherwise. The choice for κ puts the effective collision frequency approximately into the range of the lower hybrid frequency. The critical current density j_c is just above twice the equilibrium current density (GEMSUM), such that no diffusion occurs in the equilibrium. It is noted that the drift velocity of the current corresponds to about twice the Alfvén speed implying a strong source of free energy for the lower hybrid drift instability or shear driven instabilities like sausage or kink modes. We will refer to resistivity models as model 1, 2, and 3. Boundary conditions are periodic in the z direction and closed at $x = x_{\max}$ as formulated for this particular configuration in (GEMSUM).

3. Results

3.1. Numerical Limitations

Many studies of magnetic reconnection are carried out in a manner different from the approach taken in this reconnection challenge [e.g., *Petschek*, 1964; *Lee*, 1995]. Usually inflow and/or outflow boundary conditions are specified in an attempt to create steady state magnetic reconnection geometry. In the case considered here, the initial configuration is not in equilibrium neither is it attempted to create a steady state reconnection geometry.

The initial configuration is chosen as an equilibrium current sheet with a magnetic perturbation superimposed. This initial perturbation creates unbalanced $\mathbf{j} \times \mathbf{B}$ forces which accelerate the plasma in the current sheet away from the X line. Without a reconnection electric field at the X line, the resulting flow tends to evacuate the current sheet in the vicinity of the X line and thereby leads to a contraction of the current sheet and an increase of the current density at the X line. *Birn and Heese* [this issue] show an example of this situation.

The magnetic perturbation used for this problem corresponds to an amplitude of 0.1 or a normal magnetic field of $B_x = 0.04$. While this appears small, one has to keep in mind that this force can accelerate the flow to Alfvén speed in ~ 25 dynamic times. Thus this force is central to initiate and drive magnetic reconnection.

One set of the cases considered in this study makes use of a constant resistivity. This can be challenging in view of the following considerations. The reconnection rate $E_{\rm rec}$ is given by $E_{\rm rec} = \eta j_{xl}$, with a resistivity η and a current density j_{xl} at the X line. Thus the required current density is $j_{xl} = E_{\rm rec}/\eta$, and the half width of this current is $d = 1/j_{xl} = \eta/E_{\rm rec}$. In order to avoid diffusion of the magnetic field, a large Lundquist number $R = 1/\eta$ is required. However, for a large reconnection electric field, this implies a very small width for the current at the X line which has to be resolved numerically in order to resolve the relevant physics. The example of $\eta = 10^{-3}$ requires a grid separation of the order of 10^{-3} to resolve the current with a few grid spacings.

Taking into account that most methods are explicit, the required time step has to be $\Delta t \leq 0.001$ for the MHD case implying several 10^4 integration steps. For the case of whistler dynamics (Hall MHD, two fluid, and hybrid simulations) the increasing phase speed of the whistler waves with decreasing wave length (and grid resolution) requires a time step of a fraction of $(\eta/E_{\rm rec})^2$ or of order 10^{-6} for the chosen example. We note that finite electron inertia limits the whistler

phase velocity but would still imply a time step significantly smaller than for a corresponding MHD computation.

Figure 1 shows an example of the outlined problem for the case of Hall MHD with a constant resistivity of 0.01. The resolution of the grid along the x direction is $\Delta_x = 0.035$ at $x = 0$ and $\Delta_z = 0.12$ uniform in z. Figure 1a shows the distance between the dominant X and O lines (solid) and the number of X lines (dashed) in the system. Figure 1b shows the current density at the X (solid) and O line (dashed); Figure 1c shows the reconnected magnetic flux by direct integration (solid) and by integrating the reconnection electric field (dashed); and Figure 1d shows the reconnection electric field $E_{\rm rec} = E_{xl} - E_{ol}$ (solid) and the reconnection rate determined from the reconnected magnetic flux (dashed). At later times the plots of the reconnected flux and of the reconnection rate show a discrepancy between the reconnection electric field and the reconnection rate determined from the magnetic flux. It is therefore concluded that in this case, numerical dissipation must significantly add to the actual physical dissipation. The reason for this is likely a lack of resolution because the reconnection rate would require a larger current density and thus better resolution than assumed. Note that for this case, a higher spatial resolution lead to strongly enhanced turbulence.

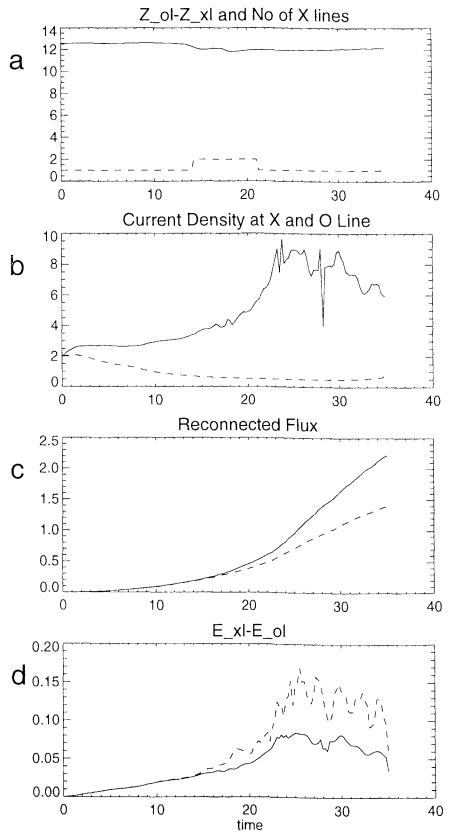

Figure 1. Typical properties for the case of a constant resistivity $\eta = 0.01$ in the Hall model are shown. (a) The distance of the dominant X and O lines (solid) and the number of X lines (dashed), (b) the current density at the X (solid) and O line (dashed), (c) the reconnected magnetic flux by direct integration (solid) and by a time integral of the reconnection electric field (dashed), and (d) the reconnection electric field (solid) and the reconnection rate determined from the reconnected magnetic flux (dashed) are shown.

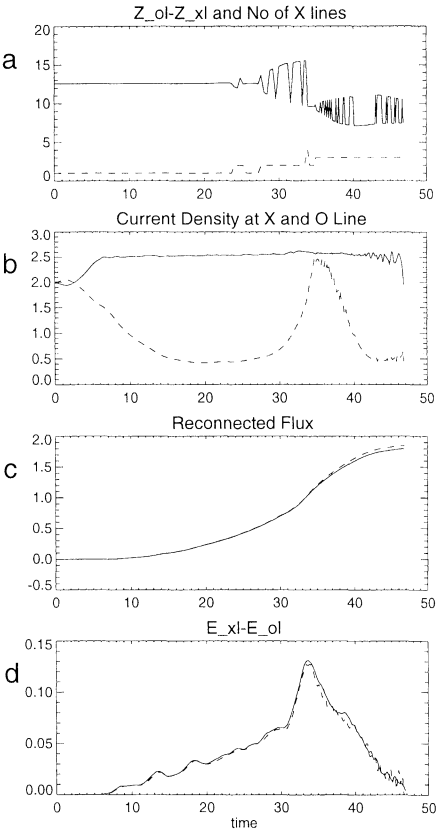

Figure 2. Same as Figure 1 for the current dependent resistivity model 1 in the MHD simulation.

It should be emphasized that the above limitations in terms of the grid spacing and the time step apply to all plasma approximations which rely on a constant resistivity to model the electric field at the X line. This includes most hybrid models, two fluid models unless the electric field is due to the electron inertial term, the Hall MHD approximation, and a less restrictive time step to MHD models.

The above reasoning changes entirely for current dependent resistivity models of the type $\eta(j) = \kappa(j - j_c)^\lambda S(j - j_c)$. In these models the dissipation is switched on only if the current density surpasses a critical current density j_c. Thus finite diffusion of the equilibrium field does not occur if the critical current is higher then the maximum current of the initial configuration. The electric field at the X line is given by $E_{\rm rec} = \kappa j_{xl}(j_{xl} - j_c)^\lambda S(j_{xl} - j_c)$. Thus a moderate increase of the current density can lead to a large increase of the reconnection rate because of the nonlinear current dependence and thereby avoiding the collapse of the current to an extremely thin layer.

An example for the limitation of the magnitude of the current density is shown in Figure 2 illustrating the same properties as Figure 1 for the case of the current dependent resistivity model 1. In this case the reconnection rate and the reconnected field agree well (with a deviation in the recon-

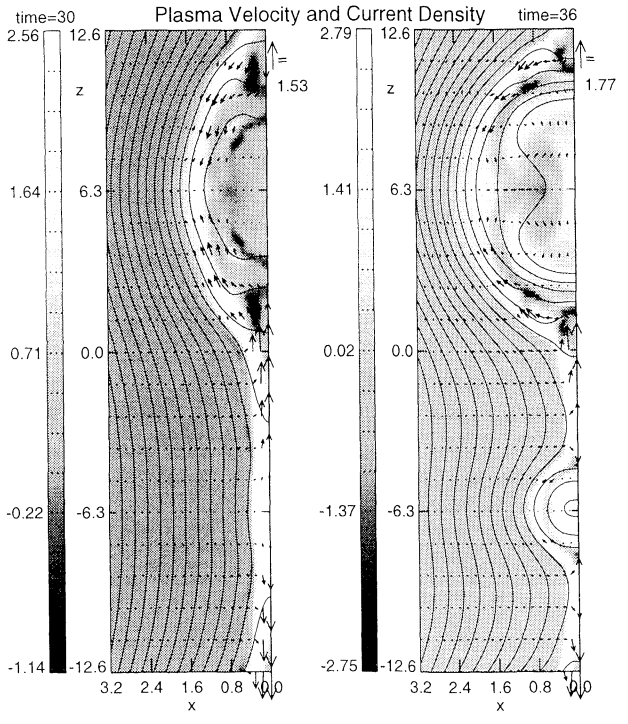

Figure 3. Plasma velocity (arrows), magnetic field lines, and current density (grey scale) for the current dependent resistivity model 1 in the MHD simulation for the times $t = 30$ (left) and 36 (right).

nected flux of $\sim 3\%$) such that numerical diffusion is negligible. We can therefore conclude that this simulation captured key aspects of the reconnection process in this MHD approximation well. Figure 2 illustrates that the current density at the dominant X line is fairly limited throughout the simulation. The results in Figure 2a also illustrate that the system develops several X lines during the evolution.

This and the larger width of the current in the diffusion region is confirmed by the result of Figure 3 showing the bulk plasma (ion) velocity (arrows), magnetic field (lines), and current density (grey) for times $t = 30$ and 36. The region of high current density at the X lines has a width of ~ 0.4 ion inertia lengths consistent with the chosen critical current density.

The current dependence and onset condition in the resistivity reflect the scattering of electrons by the turbulent wave fields of micro-instabilities such as ion acoustic, lower hybrid, ion cyclotron, and others [e.g., *Sagdeev and Galeev*, 1969; *Papadopoulos*, 1977; *Treumann and Baumjohann*, 1997]. The current dependence of the resistivity may also be of importance for whistler turbulence in reconnection because the corresponding dissipation scales with a higher order of the wave number [*Birn et al.*, this issue; *Shay et al.*, this issue].

3.2. Influence of the Initial Perturbation

As outlined above the initial perturbation acts as a driver for the plasma flow and thus may be expected to influence the reconnection process. Figure 4 illustrates results for constant resistivity of $\eta = 0.01$ and MHD dynamics with different values for the initial perturbation. We have used a flux perturbation of 0.05, 0.1 (the default configuration), 0.2, and 0.4. Figure 4a shows the reconnected magnetic flux for these cases as a function of time. Figure 4b illustrates the corresponding reconnection rate. For all cases, reconnection rates and reconnected magnetic flux are in excellent agreement (the error for the reconnected flux is $\sim 1\%$). The plots demonstrate that the perturbation has a clear influence on the evolution of the reconnection rate and on the maximum reconnection rate. Note that the fluctuations in the system are caused by fast waves due to a deviation from total pressure balance of the initial perturbation. The amplitude of the wave scales with the initial perturbation which causes larger fluctuations for the cases of higher initial perturbation. Without illustration we note that the influence of the initial perturbation on the reconnection process decreases for larger resistivity because effects of finite diffusion start to dominate the reconnection process.

Figure 5 illustrates the reconnected flux and the reconnection rate for three different perturbation levels (0.05, 0.1, and 0.2) for Hall MHD with a current dependent resistivity (model 1). Figure 5a illustrates a fast increase of the reconnected flux for a larger perturbation. The reconnection rate appears to peak also at a somewhat higher level; however, the difference in the reconnection rate is not significant compared to the fluctuations. The error for the reconnected magnetic flux compared to the integrated reconnection electric field is small for the perturbations 0.05 and 0.1 ($< 5\%$ throughout the runs) and is close to 10% for the perturbation amplitude 0.2. In general, we found all Hall MHD cases with a larger initial perturbations to be more unstable. We

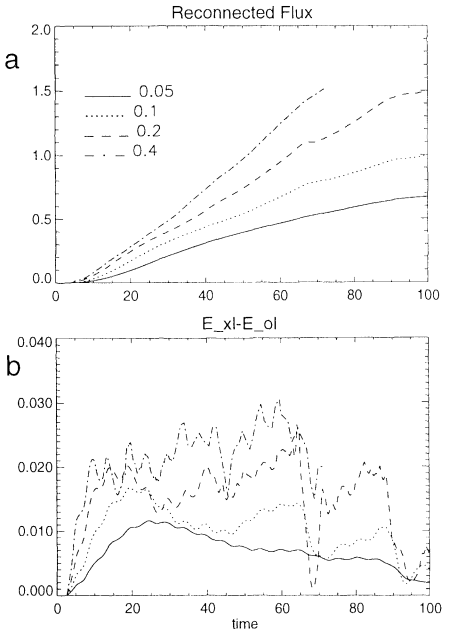

Figure 4. Reconnected magnetic flux and reconnection electric field for constant resistivity MHD simulations with different perturbation amplitude (see text).

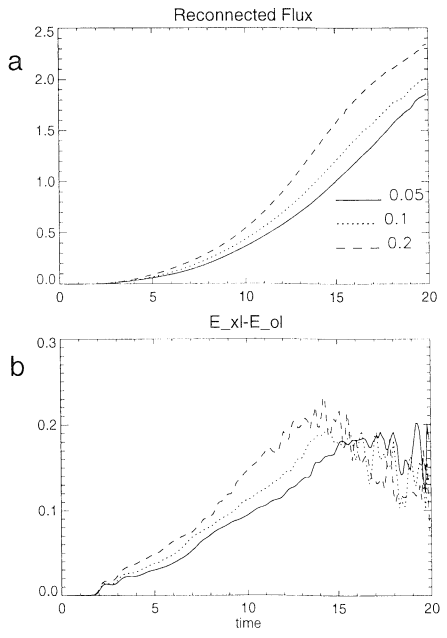

Figure 5. Same as Figure 4 for the Hall MHD cases with the current dependent resistivity model 1.

attribute this to the larger amplitude of the fast waves which may cause a higher level of whistler turbulence.

3.3. Comparison of the Different Cases

Figures 4 and 5 demonstrate that the reconnection rate depends, for the given configuration, strongly on the plasma approximation. Figure 6 compares results for the four basic models, i.e., MHD with constant resistivity, MHD with current dependent resistivity, Hall MHD with constant resistivity, and Hall MHD with current dependent resistivity. For the considered configuration the maximum reconnection rate for the MHD case with constant resistivity is obtained for $\eta = 0.02$. Thus we have chosen the same resistivity for the corresponding Hall MHD case. The current dependent resistivity is based on the model 1 both for the MHD and the Hall MHD cases.

Figure 6 demonstrates that the reconnection rate for the current dependent cases is larger than for the corresponding constant resistivity cases. The current dependent MHD case shows a maximum reconnection rate of slightly more than 0.1 which is representative (within $\sim$ 20%) for the various resistivity models and also for parameter variations such as higher or lower critical current densities or different coefficients. In most cases we also found the evolution of multiple X line as illustrated in Figures 2 and 3 for the current dependent MHD case.

While the constant resistivity in the Hall MHD approximation yields a higher reconnection rate than the corresponding MHD case, effects of finite diffusion still are present in the Hall MHD. Larger constant resistivity in Hall MHD yields lower reconnection rates because of magnetic diffusion similar to the MHD cases. However, it is quite evident that a current dependent resistivity in the Hall MHD approximation leads to significantly enhanced reconnection rates. Figure 7 shows the reconnection rates for the Hall MHD approximation using the resistivity models 1, 2, and 3. The result illustrates that the reconnection rate is indeed largely independent of the particular model.

For the case of a current dependent resistivity in the MHD simulation, Figure 2 demonstrated that a main effect of the current dependence is to determine the width of the current sheet. However, in the MHD case the resulting current sheets are relatively long with a tendency to form multiple x lines [e.g., *Biskamp*, 1986; *Lee and Fu*, 1986]. This is different in the presence of Hall physics. Figure 8 shows the plasma velocity (arrows) and current carried by ions (grey scale) on the left and the total current in the y direction on the right. Figure 9 shows electron velocity vectors and electron current (grey scale) on the left and the magnetic field B_y component on the right.

A comparison of the results in Figures 8 and 9 with Figure 3 for the MHD case shows a number of important differences. In the Hall MHD the ion current is largely just convected into the magnetic island. In the MHD case ions are accelerated at a slow shock structure [*Petschek*, 1964] just inside the separatrix, whereas in the Hall MHD case the ion velocity clearly peaks in the central outflow region and at some distance from the diffusion region (X line). This slower acceleration is caused by the ions being decoupled from the magnetic field on the ion inertia scale. In contrast the maximum velocity of the electrons occurs very close to the diffusion region with a value of just above 2 (increasing to $\sim$ 4 at $t = 20$). Away from the diffusion region the electrons are rapidly decelerated. The electrons also show

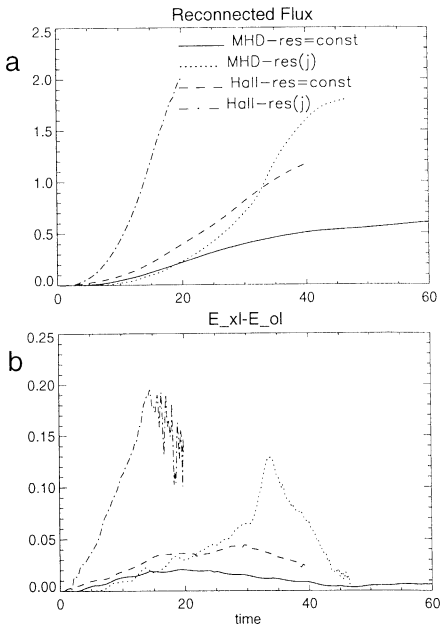

Figure 6. Same as Figure 4 for the four typical cases with constant resistivity in the MHD and Hall MHD approximations and current dependent resistivity in the MHD and Hall MHD models.

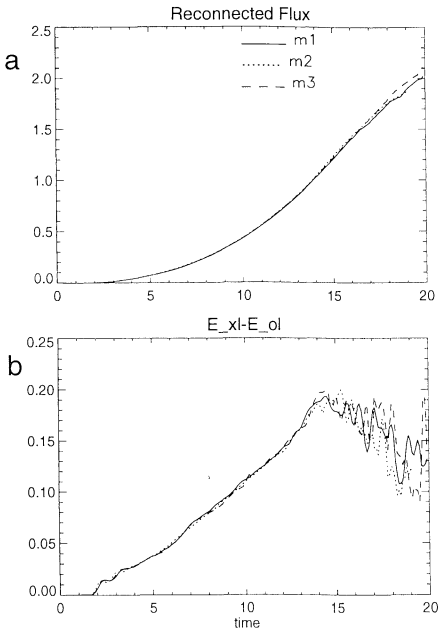

Figure 7. Same as Figure 4 for the Hall MHD runs with three different current dependent resistivity models.

a large velocity just outside the separatrix converging to the diffusion region.

The diffusion region in the Hall simulations is short (of the order of the ion inertia scale), and it is speculated that this is directly related to the whistler dynamics [GEMSUM; *Shay et al.*, this issue]. An obvious effect of the hall dynamics is the generation of a B_y component in the outflow region with a quadrupolar structure (Figure 9 only shows half of the system). This structure is determined by the electron motion out of the diffusion region and into the y direction. In the Hall approximation the magnetic field is frozen to the electron fluid (except for the diffusion region) such that a portion of a field line is carried into the y direction thereby causing the nonzero B_y component with the observed polarity.

The ion current is largely accumulated in the core of the magnetic island. However, this current is reduced by an electron current of opposite direction such that the total current in the island is significantly smaller than the ion contribution alone. Similar to the outflow region, the electron motion in the island generates a quadrupolar B_y signature. We finally note that the properties of the Hall simulation with constant resistivity are rather similar to those illustrated in Figures 8 and 9, however, with smaller velocities and B_y signatures.

4. Summary and Discussion

We have presented a comparison of results from MHD and Hall MHD computations using constant and current dependent resistivity. In all cases with a constant resistivity, magnetic reconnection proceeds at a slower rate than that for the corresponding current dependent models. A major obstacle for the use of constant resistivity is to find a proper parameter range. For a large constant resistivity, magnetic diffusion is dominating the effects of magnetic reconnection and thereby reducing the reconnection rate. For a small constant resistivity, very high spatial and temporal numerical resolution is required to model the correct physics in particular in the presence of whistler waves due to the Hall term in Ohm's law. With application to space plasma problems the use of constant resistivity can be problematic. These systems are highly collisionless such that large resistive diffusion in a simulation model is unrealistic and not suitable for such applications.

The current dependent resistivity model yields a maximum reconnection rate of 0.12 for the MHD model compared to a rate of 0.2 for the same resistivity in the Hall MHD simulation. While this difference is not really large, it is remarkable that the results for the Hall approximation are largely independent of the particular choice for the current dependent resistivity model and show very little dependence on the initial perturbation. The reconnection geometry in the Hall MHD cases is strikingly different from that for the traditional MHD in the considered cases. The diffusion region is short (of the order of the ion inertia length) and the ion flow structure deviates significantly from that seen in the MHD cases.

These results are largely consistent with results from full particle, hybrid, two fluid, and other Hall MHD models in this reconnection challenge (GEMSUM). However, even

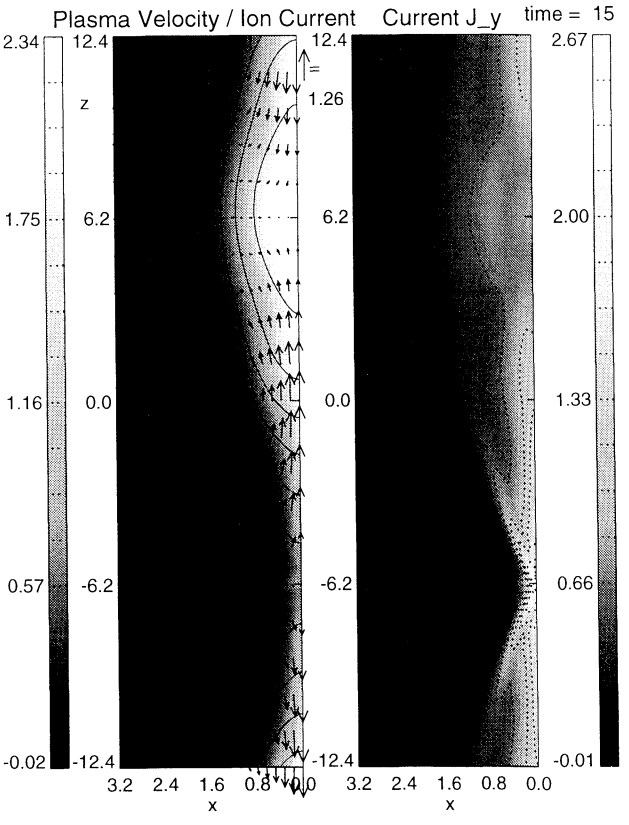

Figure 8. Two-dimensional plot of plasma velocity (arrows), magnetic field lines, and ion current density on the left and total electric current density on the right for the resistivity model 1 and Hall MHD at time $t = 15$.

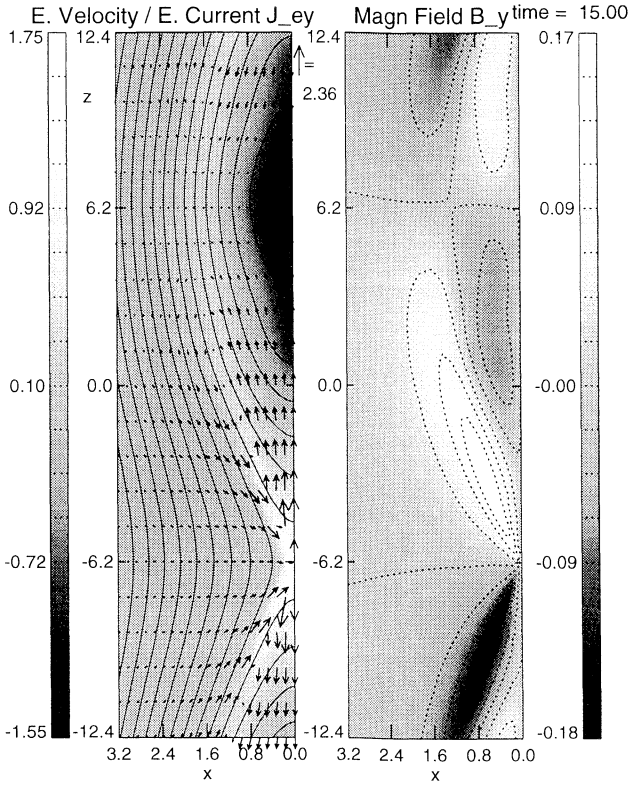

Figure 9. Two-dimensional plot of electron velocity (arrows), magnetic field lines, and electron current density (along y) on the left and the magnetic field component B_y on the right for the resistivity model 1 and Hall MHD at time $t = 15$.

though the present results agree relatively well, the results do not establish a universal reconnection rate or process. The chosen configuration is only one particular example. Unresolved questions are for instance, How does the reconnection dynamics change if the typical length scale of the configuration is much larger than the ion inertial scale? If reconnection occurs on the ion inertia scale, do large-scale structures such as magnetic flux transfer events or plasmoids contain any information on the nature of the diffusion region? The role of whistler dynamics is reduced in the presence of an initial B_y component which is typical for many space plasma currents. What are the important configurational aspects of three-dimensions and what other instabilities will play a role in three dimensions? Any of these topics may modify the present results.

Acknowledgments. The work is supported by the NASA SR&T grants NAG 5–6219 and PR 201-70856 to the University of Alaska Fairbanks. The computation is supported by Arctic Region Supercomputer Center at the University of Alaska Fairbanks.

Janet G. Luhman thanks Joachim Raeder and Terry G. Forbes for their assistance in evaluating this paper.

References

Birk, G. T., and A. Otto, A three-dimensional plasma–neutral gas–fluid code, *J. Comput. Phys.*, *125*, 513, 1996.

Birk, G. T., and A. Otto, Consequences of a resistive instability operating in the upper auroral ionosphere, *J. Atmos. Terr. Phys.*, *59*, 835, 1997.

Birn, J., Computer studies of the dynamical evolution of the geomagnetic tail, *J. Geophys. Res.*, *85*, 1214, 1980.

Birn, J., and M. Heese, Gem magnetic reconnection challenge: Resistive tearing, anisotropic pressure and Hall effects, *J. Geophys. Res.*, this issue.

Birn, J., et al., Geospace Environment Modeling (GEM) magnetic reconnection challenge, *J. Geophys. Res.*, this issue.

Biskamp, D., Magnetic reconnection via current sheets, *Phys. Fluids*, *29*, 1520, 1986.

Chen, Q., A. Otto, and L. C. Lee, Tearing instability, Kelvin-Helmholtz instability, and magnetic reconnection, *J. Geophys. Res.*, *102*, 151, 1997.

Drake, J., Magnetic reconnection: A kinetic treatment, in *Physics of the Magnetopause,* Geophys. Monogr. Ser., vol. 90, edited by P. Song, B. U. O. Sonnerup, and M. F. Thomsen, p. 155, AGU, Washington, D. C., 1995.

Hesse, M., J. Birn, and M. Kuznetsova, Collisionless magnetic reconnection: Electron processes and transport modeling, *J. Geophys. Res.*, this issue.

Lee, L. C., A review of magnetic reconnection: MHD models, in *Physics of the Magnetopause,* Geophys. Monogr. Ser., vol. 90, edited by P. Song, B. U. O. Sonnerup, and M. F. Thomsen, p. 139, AGU, Washington, D. C., 1995.

Lee, L. C., and Z. F. Fu, Multiple x-line reconnection, 1, a criterion for the transition from a single x-line to a multiple x-line reconnection, *J. Geophys. Res.*, *91*, 6807, 1986.

Ma, Z. W., and A. Bhattacharjee, Hall magnetohydrodynamic reconnection: The Geospace Environment Modeling (GEM) challenge, *J. Geophys. Res.*, this issue.

Otto, A., 3D resistive MHD computations of magnetospheric physics, *Comput. Phys. Commun.*, *59*, 185, 1990.

Otto, A., Forced three-dimensional magnetic reconnection due to linkage of magnetic flux tubes, *J. Geophys. Res.*, *100*, 11,863, 1995.

Otto, A., L. C. Lee, and Z. W. Ma, Plasma and magnetic field properties associated with pressure pulses and magnetic reconnection at the dayside magnetopause, *J. Geophys. Res.*, *100*, 14,895, 1995.

Papadopoulos, K., A review of anomalous resistivity for the ionosphere, *Rev. Geophys.*, *15*, 113, 1977.

Petschek, H. G., Magnetic annihilation, in *AAS-NASA Symposium on the Physics of Solar Flares*, edited by W. N. Hess, NASA Spec. Publ., SP-50, 425, 1964.

Potter, D. E., *Computational Physics*, John Wiley, New York, 1973.

Pritchett, P. L., Geospace Environment Modeling (GEM) magnetic reconnection challenge: Simulations with a full particle electromagnetic code, *J. Geophys. Res.*, this issue.

Sagdeev, R. Z., and A. A. Galeev, *Nonlinear Plasma Theory*, Benjamin, White Plains, N.Y., 1969.

Schindler, K., Kinematics of magnetic reconnection in three dimensions, in *Physics of the Magnetopause,* Geophys. Monogr. Ser., vol. 90, edited by P. Song, B. U. O. Sonnerup, and M. F. Thomsen, p. 197, AGU, Washington, D. C., 1995.

Shay, M. A., J. F. Drake, B. N. Rogers, and R. E. Denton, Alfvenic collisionless magnetic reconnection and Hall term, *J. Geophys. Res.*, this issue.

Sonnerup, B. U. O., G. Paschmann, and T.-D. Phan, Fluid aspects of reconnection at the magnetopause: In situ observations, in *Physics of the Magnetopause,* Geophys. Monogr. Ser., vol. 90, edited by P. Song, B. U. O. Sonnerup, and M. F. Thomsen, p. 167, AGU, Washington, D. C., 1995.

Treumann, R. A., and W. B. Baumjohann, *Advanced Space Plasma Physics*, Imperial College Press, London, 1997.

A. Otto, Geophysical Institute, University of Alaska, Fairbanks Fairbanks, AK 99775-7320. (ao@why.gi.alaska. edu)

(Received Ausgust 24, 1999; revised November 20, 1999; accepted November 22, 1999.)